REVERSE PAINTERLY RENDERING

Ying Wang and Masahiro Takatsuka
Vislab, School of IT, University of Sydney, Sydney, Australia

Keywords: Reverse Painterly Rendering (RPR), Painterly Rendering, Image Feature Extraction.

Abstract: Traditional painterly rendering algorithms transform photographic images to their artistic representations such as paintings or drawings. However, the reverse process of painterly rendering has never been discussed, which could be useful for studies in heritage and forensic science. This paper presents a novel reverse painterly rendering algorithm which restores "oil painting-like" images to photo-like images. Results show that our algorithm can improve the photorealistic appearance of "oil painting-like" images.

1 INTRODUCTION

Previously, many painterly rendering algorithms were proposed to automatically generate artistic 'painting-like' images from photographic images. However, procedures involved in these algorithms are usually non-reversible, meaning that original photographic images cannot be regenerated from rendered results. However, the reverse process of painterly rendering can be useful to some applications such as artwork restoration in heritage studies, facial reconstruction from sketch in forensic science. In case where paper based artworks need to be visualized, reverse painterly rendering can enhance the realistic appearance of painting images by transforming them into 'photograph-like' images. This paper mainly focuses on the reverse process of painterly rendering problem, and aims to develop a reverse algorithm to restore photographic images from painterly rendered images with oil painting effect. To solve reverse painterly rendering (RPR) problem, 48 image features are extracted, from which 5 key features are selected. Then an artificial neural network is trained to predict the 5 key features of the output ('photograph-like' image) from the input (painterly rendered images with oil painting effect). Using the selected key features, signal independent noise which was mainly caused by additive background texture can be removed and then we adaptively adjust the colour style and the smoothness of the contour through our selected 5 key features. Finally, the performance of our algorithm is measured against ground truth.

The rest of this paper is organized as follows: section 2 briefly reviews previous works in painterly rendering; section 3 introduces our proposed reverse painterly rendering (RPR) algorithm; section 4 presents the results of our algorithm; section 5 discusses the results; finally, section 6 concludes the paper.

2 RELATED WORKS

Previously, many "forward" painterly rendering algorithms were proposed. Typically, they take photographic images as inputs and generate images with artistic styles. Based on the rendering techniques, they can be categorized as "stroke-based" and "example-based" painterly rendering.

In stroke-based painterly rendering, an image is created by combining an ordered list of strokes described parametrically by a stroke model (Hertzmann, 2003). Haeberli was the earliest who demonstrated an interactive painting application for simulating painterly brush strokes (Haeberli, 1990). Although his application does not automate brush strokes rendering, it demonstrates the earliest idea on stroke based painterly rendering. Hertzmann formulated stroke based painterly rendering as an energy minimization problem (Hertzmann, 2001). However, solving an energy relaxation problem remains a computationally expensive task. Although some stroke based algorithms focus on rendering specific artistic styles such as impressionist (Litwinowicz, 1997) and Chinese painting (Xu et al., 2006); most of them do not explicitly have control over the rendered styles.

Wang Y. and Takatsuka M..
REVERSE PAINTERLY RENDERING.
DOI: 10.5220/0003814802410247
In *Proceedings of the International Conference on Computer Graphics Theory and Applications* (GRAPP-2012), pages 241-247
ISBN: 978-989-8565-02-0

Example-based painterly rendering algorithms present a new approach for painterly rendering. Hertzmann et al. present a novel framework called "image analogy" for transforming photos into painting-like images by examples (Hertzmann et al., 2001). In their work, painterly rendering is formulated as a problem of finding analogy. The output image is constructed by a block-wised multi-resolution synthesis. The central idea of this synthesis technique is to search for the best match image block from the examples and the input image.

In summary, stroke-based algorithms simulate the actual painting process. Since brush strokes are placed one by one on the canvas just as artists do, it is extremely difficult to derive the reverse process. Exampled-based painterly rendering algorithms produce the output by investigating and synthesizing the pixel level features of examples. However, the reverse process remains rather difficult because photographic image details are lost during the synthesis process. Although various algorithms were proposed to solve painterly rendering problem, none of them addressed its reverse process. This is particularly useful for studies in heritage and forensic science where photorealistic images of paintings may be needed. We will introduce reverse painterly rendering (RPR) algorithm in the next section.

3 REVERSE PAINTERLY RENDERING (RPR)

3.1 Problem Formulation

Assume the original photographic image is x(i,j), and its painted version is y(i,j), the problem of painterly rendering (particularly with oil painting effect) can be formulated as:

$$\mathbf{y}(i,\ j) = \mathbf{h} * (\mathbf{c} * (\mathbf{x}(i,\ j))) + \mathbf{n} \quad . \qquad (1)$$

Where **n** is signal independent noise, which are caused by adding background textures such as the texture of canvas to photographic image **x**. **c** denotes a filtering process which incurs signal dependent noise or distortion to **x**. For instance, **c** particularly causes the distortion of **x**'s edges and gradient. **h** is a 2d filter that transforms **x**'s colour style from photographic colours to painted colours , * is 2D convolution.

Therefore, the problem of RPR is to estimate the original photographic image **x** through the painterly rendered image **y**.

3.2 Solving RPR

3.2.1 Features Extraction

A number of image features are extracted. They can be categorized as: colour-related, texture-related and wavelet-related features (Table 1).

Table 1: Extracted image features.

Categories	Specific Image Features
Colour- related Features	Smoothness of colour
	Colour palette
	Colour saturation
	Prevalent colour coverage
Texture-related Features	Global Gabor filter responses
	Local Gabor filter responses
Wavelet-related Features	First order statistics of first scale wavelet sub-band coefficients

In colour-related features, *Smoothness of colour* presents the spatial variation of colour in an image plane. *Colour palette* accounts for the number of unique colours in an image. *Colour saturation* is the saturation of pixel colours indicated by H channel in HSV colour space. We extract above three features using methodology described by (Cutzu et al., 2005). *Prevalent colour coverage* presents the coverage of the most frequently appearing colour in an image, which was used to distinguish photographs from graphics on the web in (Athitsos et al., 1997).

Following the methodology introduced by (Bianconi and Fernandez, 2007), we extract texture features using statistics of Gabor filter responses at five different scales and four different orientations. *Global Gabor filter response* is obtained by averaging Gabor filter responses from all scales and orientations of a gray scale image. *Local Gabor filter responses* are Gabor filter responses from five different scales (0, 0.2, 0.4, 0.6, 0.8) and four different orientations $(0, \frac{\pi}{4}, \frac{\pi}{2}, \frac{3\pi}{4})$, respectively.

The four first order statistics (mean, variance, skewness and kurtosis) of wavelet sub-band coefficients were used in (Lyu and Farid, 2005) and (Wang and Moulin, 2006) to distinguish computer generated photorealistic images from real photographic images. Similarly, we adopt *first order statistics of first scale wavelet sub-band coefficients* as wavelet-related features.

All the features described above are normalized by the size of the image so that we obtain a score for each individual feature. RGB colour images are converted to greyscale images to extract texture and

wavelet related features. All the extracted features form the feature space **F.** **F** is a 48 dimensional vector, and each dimension of **F** corresponds to an extracted feature. The notation of F is defined as follows:

$$\mathbf{F} = \{f_1, f_2 \dots \dots f_{48}\} \quad . \quad (2)$$

Where

f_1: smoothness of colour
f_2: colour palette
f_3: prevalent colour coverage
f_4: global Gabor filter response
f_5~f_{10}: kurtosis and variance of 1st scale wavelet high frequency (i.e. horizontal, vertical and diagonal) components coefficients
f_{11}~f_{26}: mean, variance, skewness and kurtosis of 1st scale wavelet sub band coefficient histograms
f_{27}~f_{28}: skewness and kurtosis of colour saturation histogram
f_{29}~f_{48}: local Gabor filter responses

To testify if above features can identify the differences between photographic images and "oil painting-like" images, we build a Support Vector Machine (SVM) classifier using above features to distinguish photographic images from "oil painting-like" images. We first obtain an image dataset (Martin, 2001) containing 500 photographic images and then apply "oil painting effect" to the entire dataset in Photoshop. Totally, 1000 images (500 photographic images and 500 painterly rendered images) are obtained. Then, we extract features defined in formula (2) from obtained image pairs. Finally, we use 700 images for training SVM to label them as either "photo" or "painting", and 300 images for test.

The accuracy of the classification is 0.91. Therefore, we conclude that features defined in formula (2) are able to characterize the differences between photographic images and "oil paint-like" images.

3.2.2 Key Features Selection and Prediction

Among all the obtained 48 image features, we want to further select the key features that contribute most to the classification result. We use t-test (Guyon and Elisseeff, 2003) to assess the significance of each feature for separating two labelled groups ("photo" and "painting"). Table 2 shows 10 highest ranked features.

In Table 2, the top 5 key features are: f_2, f_4, f_{46}, f_{48}, f_{42} (see formula (2) for definition).

Table 2: List of ranked features by t-test.

10 highest ranked features	Feature category	T-test scores
f_2	Colour-related	19.8797
f_4, f_{46}, f_{48}, f_{42}, f_{44}, f_{38}	Texture-related	18.2364~ 12.9264
f_{12}, f_{10}, f_{17}	Wavelet-related	12.6664~ 11.9440

We then use 5 highest ranked features to train the SVM classifier again. The accuracy of the classification is 0.82, proving that the 5 highest ranked features (out of 48 features) are able to represent the entire feature set.

To reverse an "oil painting-like" image to a "photo-like" image, we need to predict the above 5 key features of the original photographic image. Artificial neural network was used for the prediction. We use the same image dataset to train a back propagation neural network with key features of 350 image pairs (i.e. 350 painterly rendered images as inputs, 350 photographic images as targets). 150 image pairs are used for test. Table 3 shows Mean Squared Error (MSE) of predicted 5 key features.

Table 3: MSE of predicted key features.

Features	f_2	f_4	f_{46}	f_{48}	f_{42}
MSE ($\times 10^{-3}$)	3.1	6.1	5.5	5.4	5.6

Given an "oil painting-like" image as input, the output of our RPR algorithm should be an image whose key features are close to the key features of the photographic image.

3.2.3 Signal Independent Noise Removal

Based on formula (1), the additive noise **n** needs to be removed. The cause of **n** is primarily from adding a background texture such as canvas to an image, therefore **n** is independent from **x**. We assume **n** has constant variance which can be estimated by feature f_4: *global Gabor filter response*. 2D adaptive wiener filter is used for noise removal. At each pixel point y(i, j), we calculate the local mean and local variance of y(i, j) within its neighbourhood, and then the following formula is applied to reduce the noise:

$$y_1(i,j) = \text{mean}_l + \frac{\text{var}_l - \text{var}_n}{\text{var}_l}(y(i,j) - \text{mean}_l) \; . \quad (3)$$

Where mean_l and var_l are local mean and local variance of pixel point y(i, j) within its neighbourhood. $\mathbf{y_1}$ is the result image. var_n is the variance of the signal independent noise estimated by *Global Gabor filter response* (feature f_4). The result of applying this filtering to a painterly

rendered image is shown in Figure 1(b).

3.2.4 Colour Style Adjustment

In formula (1), the effect of 2D colour filtering **h** needs to be reversed. To adjust the colour style, we make use of the highest ranked feature f_2: *colour palette*. First, we convert the image $\mathbf{y_1}$ in formula (3) from RGB to HSV colour space. Then 2D LMS (Least Mean Square) algorithm is applied to the saturation channel of the image $\mathbf{y_1}$. After the process, the image is converted back to RGB colour space. At each iteration,

$$\mathbf{y'_{1saturation}}(i,j) = \sum_{i=1}^{m}\sum_{j=1}^{n} w(i,j)\, y_{1saturation}(i,j) \quad . \quad (4)$$

$$\mathbf{w}(i,j) = \sum_{i=1}^{m}\sum_{j=1}^{n}\left(w(i,j) + err \times y_{1saturation}(i,j)\right) \quad . \quad (5)$$

$$err = r \times (\text{predicted } f_2 - \text{current } f_2) \quad . \quad (6)$$

Where m and n are the height and width of the image $\mathbf{y_1}$. **w** is a 2D weight mask used for filtering. r is a constant that controls the learning rate. This colour filtering process will run iteratively until error is less than 0.01. The result of colour style adjustment is shown in Figure 1(c).

3.2.5 Contour Smoothing

Finally, we need to reduce signal dependent distortion **c** in formula (1). From our observation, **c** primarily causes the jerkiness of edges and the uneven changes of colour (i.e. gradient) in an image. In the feature space, **c** causes the differences between painterly rendered images and photographic images in local Gabor filter responses, i.e. f_{46}, f_{48} and f_{42}. The effect of **c** can be alleviated by iteratively smoothing the contour of the image. Since LUV colour space separate image luminance from colour, we smooth the image contour in each channel of LUV colour space. We first extract the edges of an image. Then we remove small objects from the edges and smooth the remaining edges using local regression. For each point on the remaining edges, we sample its N neighbouring points on each side and a local regression line is computed. Then the current point is projected on this line. The result of smoothed edges is shown in Figure 1(f).

After we obtain the smoothed edge (e.g. Figure 1(f)), we use it to smooth image contour obtained from colour style adjustment (e.g. Figure 1(c)). We first convert the image to LUV colour space. For each channel, we calculate the gradient towards horizontal direction and vertical direction. And the gradient map is the magnitude of the gradient, i.e.

$$\text{Gradient Map} = \sqrt{\nabla x^2 + \nabla y^2} \quad . \quad (7)$$

Where ∇x and ∇y are image gradient toward horizontal and vertical directions.

For each pixel in the image, if it is on both of the original edges (e.g. Figure 1(e)) and the smoothed edges (e.g. Figure 1(f)), we leave it unchanged. If it is on the original edges but not on the smoothed edges, we change the pixel value to the value of its nearest neighbouring pixel that has the minimum gradient indicated by gradient Map. Similarly, if it is not a on the original edges but on the smoothed edges, we change the pixel value to the value of its nearest neighbouring pixel that has the maximum gradient indicated by gradient Map. We run this smoothing algorithm iteratively until local Gabor filter responses (f_{46}, f_{48} and f_{42}) are close to the predicted values. The final result of applying contour smoothing is shown in Figure 1(d).

3.2.6 Algorithm

The work flow of RPR algorithm is summarized in a chart (Figure 2). Our algorithm first extracts potential features for classifying the image data set (section 3.2.1).Then based on the classification result, we select and predict five key features to control the process of RPR (section 3.2.2). Given the input painterly rendered image, we first remove the signal independent noise (section 3.2.3); then adjust the colour style (section 3.2.4) and smooth the contour (section 3.2.5) to obtain the restored photograph-like image.

4 RESULTS

4.1 Experimental Data

To acquire image pairs for our experiment, we download UC Berkley image segmentation dataset (Martin, 2001) which contains 500 photographic images of various subjects. The sizes of these images are either 481×321 or 321×481. Then we use Photoshop to apply oil painting effect to the entire dataset. Eventually, a total number of 1000 images containing 500 original photographic images and 500 painterly rendered images are obtained.

4.2 Experimental Result

Figure 3 shows our RPR result compared with ground truth images. In Figure 3, Column A (left) is

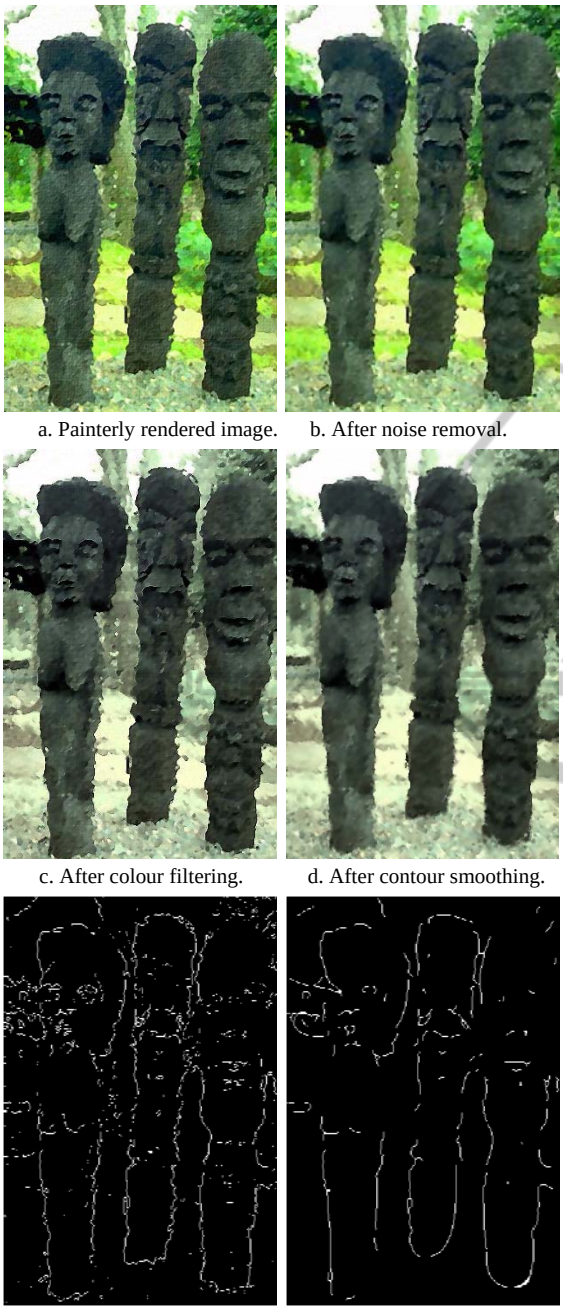

a. Painterly rendered image. b. After noise removal.

c. After colour filtering. d. After contour smoothing.

e. Original edges. f. Smoothed edges.

Figure 1: Three step process of RPR algorithm.

images with oil painting effect; Column B (middle) is the photo-like images restored by our RPR algorithm; Column C (right) is the original photos. Images of column A are obtained by applying oil painting effect to column C in Photoshop. Therefore, column C can be used as ground truth for measuring the performance of the result.

4.3 Performance

We first compare the absolute image difference ($D_{restored\text{-}orignal}$) between our restored photographic images and the original photographic images with the difference ($D_{painting\text{-}orignal}$) between the painterly rendered images and the original photographic images. Since LUV colour space separates luminance from colour, we calculate the average pixel-wised absolute difference through three channels in LUV colour space. Table 4 are $D_{restored\text{-}orignal}$ and $D_{painting\text{-}orignal}$ of images shown in Figure 3.

Table 4: Comparison of the image differences in Figure 3.

	$D_{restored\text{-}orignal}$	$D_{painting\text{-}orignal}$
1st row of Figure 3	3.6906	6.4089
2nd row of Figure 3	2.5018	4.2270
Average	3.0962	5.3180

From Table 4, we can see that our algorithm manages to reduce the pixel-wised image difference between painterly rendered images and photographic images.

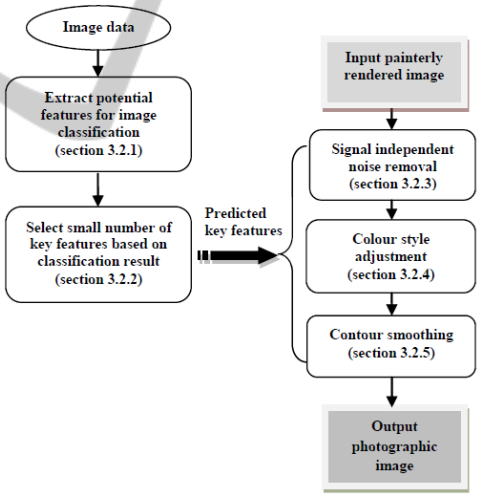

Figure 2: The workflow of RPR algorithm.

Furthermore, we compared the five key features (f_2, f_4, f_{46}, f_{48}, f_{42}) of our experimental result shown in Figure 3. Figure 4 is the comparison results. To measure the differences of key features shown in Figure 4, we can calculate the Euclidean distances between predicted and original key features, key features of our restored and original photos, key features of painterly rendered images and original photos. In Figure 4, key features of restored photograph-like images are closer to the original photographs than "oil painting-like" images. In the feature space, our algorithm manages to reduce the

A. Painterly rendered images. B. Restored photographs by RPR. C. Original photographs.

Figure 3: Results of Reverse Painterly Rendering (RPR).

Euclidean distance between key features of painterly rendered images and photographic images.

From measuring the pixel-wised image difference and Euclidean distances of key features, we can conclude that our RPR algorithm indeed improves the visual realistic appearance of painterly rendered images by reducing the pixel-wised difference and distance of key features from their original photographic images.

5 DISCUSSION

From the results, we can see that our RPR algorithm manages to reduce the differences between "oil painting-like" images and true photographic images. However, our restored images are still visually different from photographic images. Especially when the original photographs have more detailed regions (such as trees or grass), our algorithm does not perform very well. This is because important image details are lost or distorted during the forward process of painterly rendering. Furthermore, since the distortion of image edges and gradient in the process of painterly rendering is still not well studied, our contour smoothing algorithm remains to be improved. Additionally, our painterly rendered images are limited to the "oil painting effect" in Photoshop; this is because we found the "oil painting effect" generated by Photoshop is closer to oil paintings produced by human artists than any other software such as Irfanview or Paint shop pro. However, in the future, we would still like to work on real oil paintings of various styles and particularly study how contours of objects in oil paintings are differentiated from photographs. Meanwhile, image super-resolution and synthesis technique may be adopted to recover the details of photographic images.

6 CONCLUSIONS

In this paper, we present a novel RPR algorithm which can reverse the painterly rendered images (with oil painting effect) to photograph-like image. We first formulate the process of painterly rendering with oil painting effect; then to reverse the process, we extract important image features through classifying photographic images from their painterly rendered images; removing signal independent noise; adjusting colour style and smoothing contours. Finally, we measured the performance of our RPR algorithm. The result shows that our algorithm is able to improve the photo-realistic appearance of "oil painting-like" images.

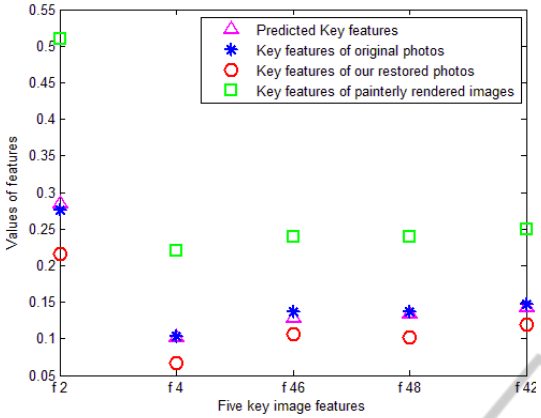

a. Key features of images in 1st row of Figure 3.

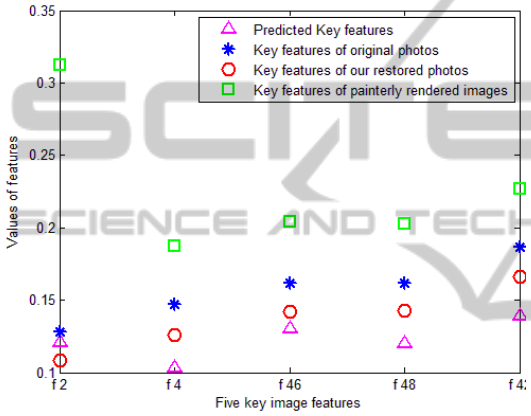

b. Key features of images in 2nd row of Figure 3.

Figure 4: Comparison of five key image features.

REFERENCES

Athitsos, V., Swain, M. J., Frankel, C., 1997. Distinguishing Photographs and Graphics on the World Wide Web. *IEEE Workshop on Content-Based Access of Image and Video Libraries, 1997.*

Bianconi, F. and Fernandez, A., 2007. Evaluation of the Effects of Gabor Filter Parameters on Texture Classification. *Pattern Recognition 40 (2007), page 3325-3335.*

Cutzu, F., Hammoud, R. and Leykin, A., 2005. Distinguishing Paintings from Photographs. *Comput. Vis. Image Understanding, vol.100, no. 3, page 249-273.*

Guyon, I. and Elisseeff A., 2003. An Introduction to Variable and Feature Selection. *Journal of Machine Learning Research 3(2003), page 1157-1182.*

Haeberli, P., 1990. Paint by Numbers: abstract image representations. *SIGGRAPH Comput. Graph. page 207-214.*

Hertzmann, A., 2001. Paint by Relaxation. *Proceedings of Computer Graphics International (CG1). page. 47-54.*

Hertzmann, A., Jacobs, C. E., Oliver, N., Curless, B. and Salesin, D. H., 2001. Image Analogies. *Proceedings of the 28th annual conference and computer graphics and iteractive techniques.*

Hertzmann, A., 2003. Tutorial: A Survey of Stroke-Based Rendering. *IEEE Comput. Graph. Appl., vol.23, no.4, 2003, page 70-81.*

Litwinowicz, P., 1997. Processing Images and Video for an Impressionist Effect. *Proceedings of the 24th annual conference on computer graphics and interactive techniques. page 407-414, ACM Press/Addison-Wesley Publishing Co.*

Lyu, S., Farid, H., 2005. How realistic is photorealistic? *IEEE Transactions on Signal Processing, vol.53, no.2, page 845- 850.*

Martin, D., Fowlkes, C., Tal, D., Malik, J., 2001. A Database of Human Segmented Natural Images and its Application to Evaluating Segmentation Algorithms and Measuring Ecological Statistics. *Proceedings of the 8th International Conference on Computer Vision (ICCV).*

Wang Y., Moulin, P., 2006. On Discrimination Between Photorealistic and Photographic Images. *Proceedings of 2006 IEEE International Conference on Acoustics, Speech and Signal Processing.*

Xu, S., Xu, Y., Kang, S. B., Salesin, D. H., Pan, Y., and Shum, H.-Y. 2006. Animating Chinese Paintings Through Stroke-based Decomposition. *ACM Trans. Graph. vol.25, no. 2, page 239–267.*